

Bi-Directional Static Load Testing Results of an Augered Cast-In-Place Pile and a Drilled Displacement Pile

Seth O. Robertson, Ph.D., P.E., M.ASCE,¹ Marty G. Bixler, P.E., M.ASCE,² and Van E. Komurka, P.E., D.GE, F.ASCE³

¹GRL Engineers, Inc., 30725 Aurora Rd, Cleveland, Ohio 44139; e-mail:
SRobertson@GRLEngineers.com

²GRL Engineers, Inc., 23015 SE 270th St, Maple Valley, WA 98038; e-mail:
MBixler@GRLEngineers.com

³GRL Engineers, Inc., 30725 Aurora Rd, Cleveland, Ohio 44139; e-mail:
VKomurka@GRLEngineers.com

ABSTRACT

Augered cast-in-place (“ACIP”) piles and drilled displacement piles (“DDP”) are becoming increasingly common, particularly for providing high bearing capacities with relative ease of installation, reduced overall costs, and potential for shortened construction schedule and reduced construction material quantities. The static analysis methods used for these methods’ designs contain uncertainties, particularly for DDP where the surrounding geomaterials are reformed, resulting in increased unit side-shear resistance. Load testing is often performed to assess the side-shear and end-bearing resistances, and to evaluate the selected construction method and required pile lengths. Bi-directional static load testing (“BDSLTL”) can be advantageous for determining mobilized side-shear and end-bearing resistances at lower cost compared to conventional top-loading static load tests. A case study is presented where an ACIP pile and a DDP were constructed in close proximity to each other, and both were bi-directionally load tested. The benefits and limitations of each foundation type are addressed. A comparative study of load test results is presented showing the response of each pile type in similar subsurface conditions. Critical aspects of the test data and their interpretation are reviewed, focusing on fundamental aspects of performing a BDSLTL, and methods applicable to converting measured strain to calculated internal force for drilled deep foundations. Higher mobilized side-shear resistances were observed for the DDP, which exhibited 50 to 100% greater resistance compared to the ACIP pile in dense deposits. However, limitation in the DDP construction method (manifested as relatively shallow drilling-tool refusal) was encountered, limiting the DDP maximum achievable total capacity.

INTRODUCTION

A critical component of deep foundation design is the appropriate selection of the most-desirable foundation type and construction method, tailored to satisfying load-resistance demands, cost efficiency, and site-specific subsurface conditions. Drilled deep foundations are often advantageous for providing high bearing capacities, particularly when installed in dense soil,

intermediate geomaterials, or weathered rock. Augered cast-in-place (“ACIP”) piles and drilled displacement piles (“DDP”) are becoming increasingly common types of drilled deep foundations. These pile installation methods provide high bearing capacities with relative ease of installation, reduced overall costs, and potential for shortened construction schedule and reduced construction material quantities.

Drilled displacement refers to a special class of piles which incorporate a specially designed helical auger segment to laterally displace soil as the auger is advanced, thus acting as a means of ground improvement, resulting in increased soil (and therefore side shear) resistance compared to ACIP piles. The displaced soil also reduces the amount of drill cuttings, offering significant cost savings in certain subsurface conditions or contaminated soils. The displacement auger is commonly advantageous in clean, loose sands with shallow groundwater, a condition which is unfavorable for continuous flight augers. However, DDP require much greater torque than ACIP piles in dense granular materials, cemented soils, or weak rock, conditions favorable for ACIP piles (Basu et al., 2010; Brown, 2012; Brown et al., 2007). Figure 1 displays the DDP drilling rig used for the case study presented herein.

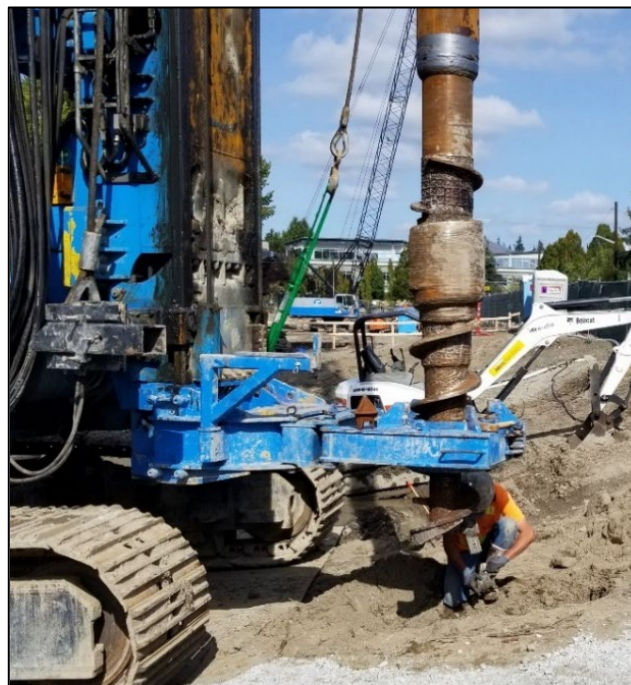


Figure 1. DDP drilling rig used on the project.

Comparative studies between the ACIP and DDP installation methods have shown DDPs can significantly increase the side-shear resistance (Brown et al., 2007; Park et al., 2011). However, the accuracy of static analysis methods used to predict capacities for these installation methods (particularly for DDP where surrounding geomaterials are heavily disturbed) varies significantly depending on soil type and quality of installation procedures. Load testing is often performed to assess the side-shear and end-bearing resistances, and to evaluate the selected construction method and required pile lengths. Bi-directional static load testing (“BDSL”) is particularly advantageous for computing mobilized side-shear and end-bearing resistances at lower cost compared to

conventional top-loading static load tests. BDSLT incorporates a hydraulic jack embedded within the foundation element, commonly at a selected depth intended to result in equal resistance above and below the jack assembly, therefore targeting maximized total measured resistance.

Uncertainty arises in the BDSLT interpretation due to the inherent assumption that soil resistance is independent of the applied load direction, as well as differences in pile-end conditions during load testing versus during service loads' application. Additionally, if the embedded jack is not located at or near the resistance balance point, the nominal geotechnical resistance cannot be fully mobilized.

Embedded instrumentation such as displacement transducers, strain gages, and thermal wire are often incorporated in BDSLT to measure the required test parameters for subsequent interpretation of displacements, elastic compressions, internal forces, and mobilized side-shear, end-bearing, and total resistances. Strain gages ("SG") are typically fixed directly to the longitudinal reinforcing bars at locations bounded by substrata of interest, or spaced equally along the embedded pile length. From measured internal pile strain, ϵ , the internal force, F , can be determined if the pile properties are known (i.e., $F = \epsilon E_{PILE} A_{PILE}$, thus the pile's composite modulus of elasticity, E_{PILE} , and total cross-sectional area at that location, A_{PILE} , must be reasonably estimated). Thermal Integrity Profiling can assist in determining the as-built pile geometry, given detailed and accurate installation records, and owing to the fact drilled foundations are very often non-uniform (Bixler et al., 2016; Komurka and Robertson, 2020). Various methods exist for estimating concrete and grout elastic modulus, and industry standards often rely on empirical correlations (i.e., ACI, 2014) based on uniaxial compression strength test results. A more-direct method of computing internal force is summarized by Komurka and Moghaddam (2020), defined as the Incremental Rigidity ("IR") method, which accounts for potential non-uniformities with depth (of both elastic modulus and cross-sectional area) via internal calibration of strain-dependent rigidity ($E_{PILE} A_{PILE}$).

A comparative study of load test results is presented to demonstrate the efficacy of each pile type bearing in dense granular glacial deposits. Critical aspects of the test data, and their interpretation, are reviewed, focusing on fundamental characteristics of performing a BDSLT, methods applicable to converting measured strain to calculated internal force, and calculated unit side-shear and end-bearing resistances.

CASE STUDY OVERVIEW

Project Description. The case study presented herein is a proposed construction of three seven-story apartment buildings, located in the Pacific Northwest.

General Subsurface Information. The subsurface strata at the project location generally consist of existing fill material overlying organic silt, overlying loose silty sand which extends 3 to 6 m (10 to 20 ft) below grade. Dense to very dense glacial deposits exist under the loose silty sand stratum, and generally consist of poorly graded sand, with gravel and silt.

Foundation Design and Construction. Augered cast-in-place piles were initially proposed for the primary structure support system, designed to resist a maximum factored axial load of 1,334

kN (300 kips) per pile. The anticipated minimum pile embedment was 13.7 m (45 ft) into the dense glacial deposits, for a total length of approximately 18.3 m (60 ft). Drilled displacement piles were alternatively proposed for potential cost savings, requiring only 9.1 m (30 ft) embedment in the dense glacial deposits, and reducing costs associated with drill cutting removal. It was recognized, however, that potential auger refusal may restrict DDP maximum achievable embedment, thereby requiring a pile-specific capacity evaluation at each pile's base elevation. Each installation method called for 45.7-cm (18-inch) -diameter piles, with a 30.5-cm (12-inch) -diameter steel reinforcing cage and full-length center bar.

LOAD TEST PROGRAM

Overview. A foundation load test program was implemented to demonstrate the efficacy of the augered cast-in-place and drilled displacement pile installation methods, and to assess the unit side-shear and end-bearing resistances for each foundation type. The designated maximum test load was 3,559 kN (800 kips), or 2.67 times the maximum axial design load. To meet these loading needs cost-effectively, bi-directional static load testing was selected. Preliminary test program requirements called for a single drilled displacement test pile, installed to approximately 18.3-m (60-ft) embedment or auger refusal, whichever was shallower. A single 2,669-kN (600-kip) embedded hydraulic jack, herein designated as a GRL-Cell, was designed to have its break plane located 3 m (10 ft) above the pile base, and to be attached directly to the 30.5-cm (12-inch) outer-diameter steel reinforcing cage. The GRL-Cell had the potential to bi-directionally load the pile to a maximum 5,338-kN (1,200-kip) test load (i.e., 2,669 kN upward and 2,669 kN downward).

The test pile was to be installed near the southern end of the project, where the poorest subsurface conditions were identified. Standard Penetration Test ("SPT") results near the test pile location indicated that uncorrected SPT-N values in the upper fill materials, organic soil, and silty sand ranged from 3 to 10 blows/30cm (3 to 10 blows/ft). The dense glacial deposits were encountered 6.6 m (21.5 ft) below grade, with SPT-N values ranging from 28 to more than 50 blows/30cm (28 to more than 50 blows/ft) (i.e., practical SPT refusal).

Drilled displacement test pile drilling began September 25, 2019; drilling refusal was experienced 8.5 m (28 ft) below ground surface. Modifications to the test pile length, GRL-Cell location, and associated instrumentation were implemented to account for the pile's shortened embedment. The bi-directional static load test was conducted one week following pile installation. Because the DDP test evidenced insufficient capacity, it was decided to install a second test pile using the ACIP method deeper than the DDP. Details of the test piles' installations, instrumentation, and load test results are discussed in the following sections. Figure 2 displays the elevation view of each test pile, and includes general subsurface conditions and locations of the embedded SG levels.

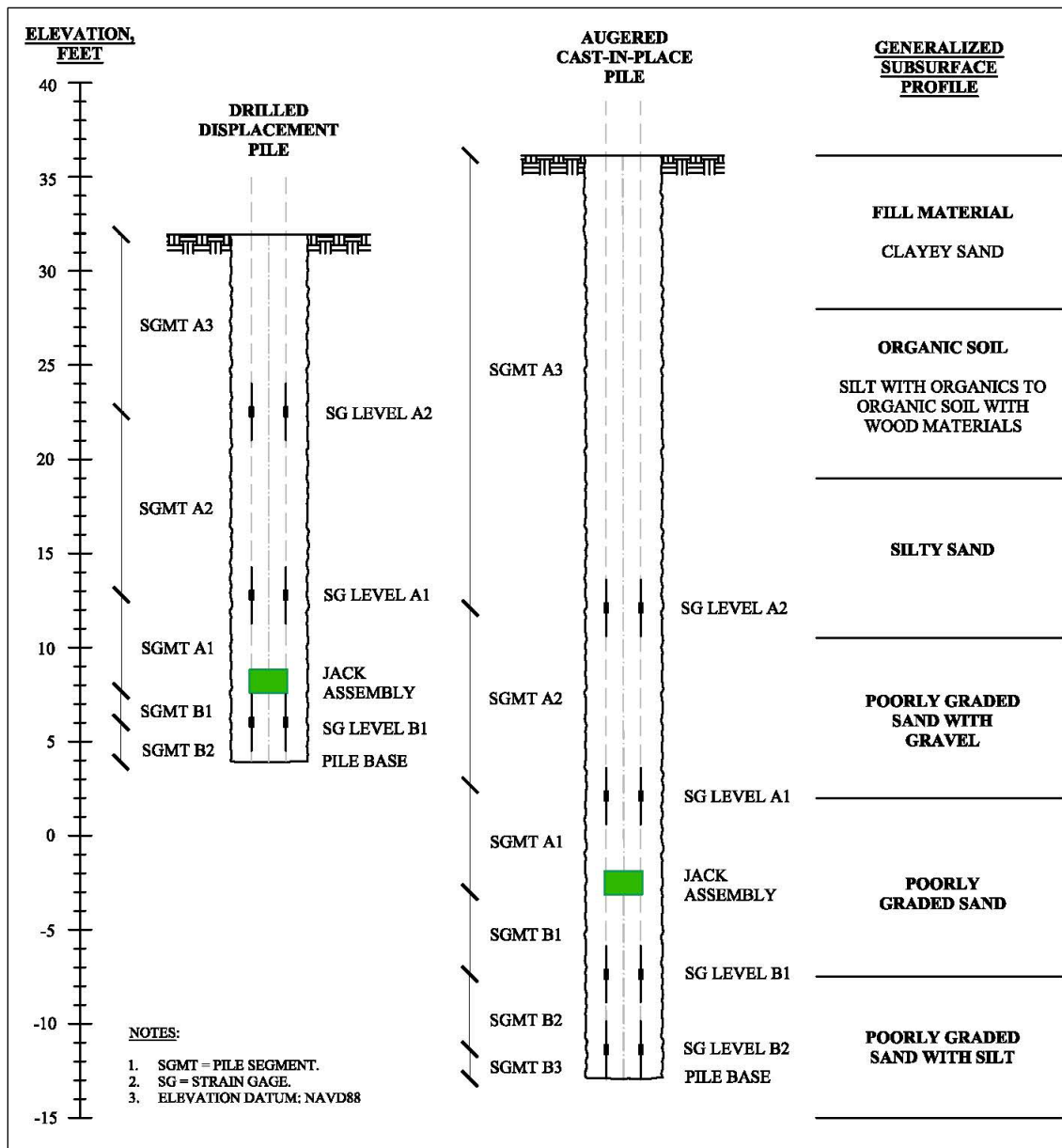


Figure 2. Pile installations elevation views.

Pile Installation Details. The test piles are designated TDDP-1 and TACIP-1. Additional fill material was placed after TDDP-1 construction and load testing, resulting in an approximately 1.2-m (4-ft) increase in ground surface elevation prior to installing TACIP-1. The 8.5-m (28-ft) long DDP was embedded 2 m (6.5 ft) into the dense glacial deposits. TACIP-1 was installed to 14.9 m (49 ft) below grade at the time of the test, resulting in a 7.1-m (23.4-ft) embedment length into the dense glacial deposits. While early auger refusal was exhibited with the DDP method, no problems penetrating the dense glacial deposits were encountered while drilling the ACIP pile.

The GRL-Cells' break planes were installed 0.9 m (3 ft) above the DDP base, and 3 m (10 ft) above the ACIP pile base. Figure 3 displays the instrumented DDP reinforcing cage, including the completed jack assembly, prior to installation in the grout-filled hole.



Figure 3. BDSLT Test Pile TDDP-1 completed jack assembly and instrumented reinforcing cage.

Uniaxial compressive strength tests were conducted on grout cylinder samples obtained during installation of each test pile. The average values of the compressive strength measured on the day of the test, f_c' , for the DDP and ACIP pile were 31.0 and 34.6 MPa (4,500 and 5,025 psi), respectively.

Instrumentation. Embedded instrumentation was incorporated in the test pile program to characterize soil response to applied test loads. The primary goal of embedded instrumentation consists of obtaining critical measurements to calculate displacements, elastic compressions, internal forces, and mobilized side-shear, end-bearing, and total geotechnical resistances. To this end, vibrating-wire displacement transducers vertically spanned across each GRL-Cell, and vibrating-wire strain gages (“sister-bar” strainmeters) were attached to the reinforcing cage above and below each jack assembly.

Each SG level consisted of two orthogonally oriented sister-bar strainmeters. SG levels nearest the pile base additionally incorporated two concrete embedment strain gages, spaced 90 degrees from the sister-bar strainmeters. Definition of “pile segments” are designated to embedded pile lengths bounded by SG levels, the pile head/base, and the jack assembly’s break plane (as shown in Figure 2).

For both test piles, Thermal Integrity Profiling (“TIP”) was implemented for assessing grout quality and evaluating geometric changes along the as-built foundation length. Two thermal wires were installed orthogonally along the full length of each reinforcing cage. These measurements offer insight into potential differences along the piles’ lengths in cross-sectional areas. In turn, these potential differences in cross-sectional areas affect axial rigidities at SG levels, which has direct application in converting measured strain to calculated internal force and unit side-shear resistances (Komurka and Robertson, 2020).

The thermal results indicated that each test pile’s estimated diameter was greater than the nominal 45.7 cm (18 inches). Enlargement of cross-sectional area was evident within the upper loose organic materials, and was subsequently utilized in the tests results’ evaluations. Pisciasko (2014) and Komurka and Robertson (2020) provide assessments of the TIP method and implementation in static load test data reduction, respectively. However, a detailed review of this case study’s TIP results extends beyond the scope of this paper.

BI-DIRECTIONAL STATIC LOAD TEST RESULTS

Overview. Conventional reporting of pile/soil response to bi-directionally applied loads may include plots of the upward and downward applied loads versus jack assembly displacement, unit side-shear and end-bearing resistances versus relative pile-soil displacement, and estimated pile-top load versus displacement under equivalent mobilized soil resistances. This section presents these results for each test pile.

GRL-Cell Load-Displacement Results. Examining GRL-Cell test load versus top and bottom displacements allows for a broad overview of mobilized side-shear and end-bearing resistances and overall pile-soil failure mechanisms. It should be noted that upward test load equals the GRL-Cell load minus the buoyant pile weight above the break plane. Downward test load is equal to the GRL-Cell load. Figures 4 and 5 present the GRL-Cell load-displacement plots for TDDP-1 and TACIP-1, respectively.

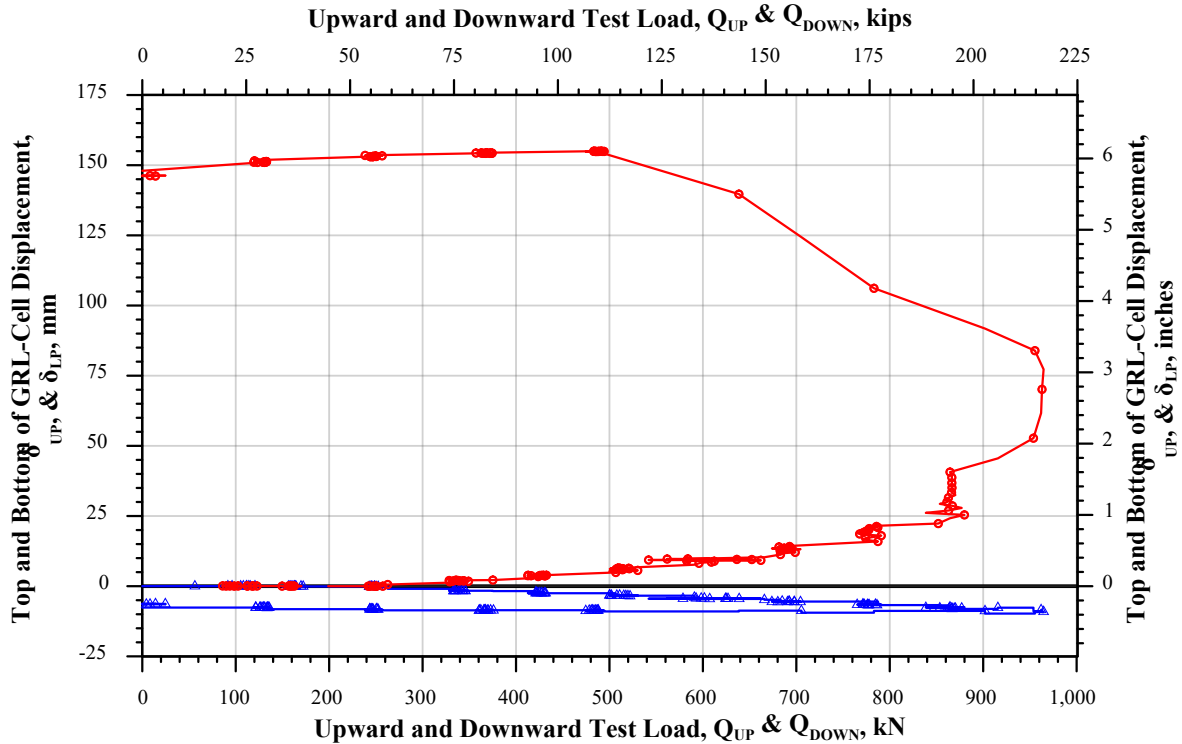


Figure 4. TDDP-1 jack assembly load-displacement plot.

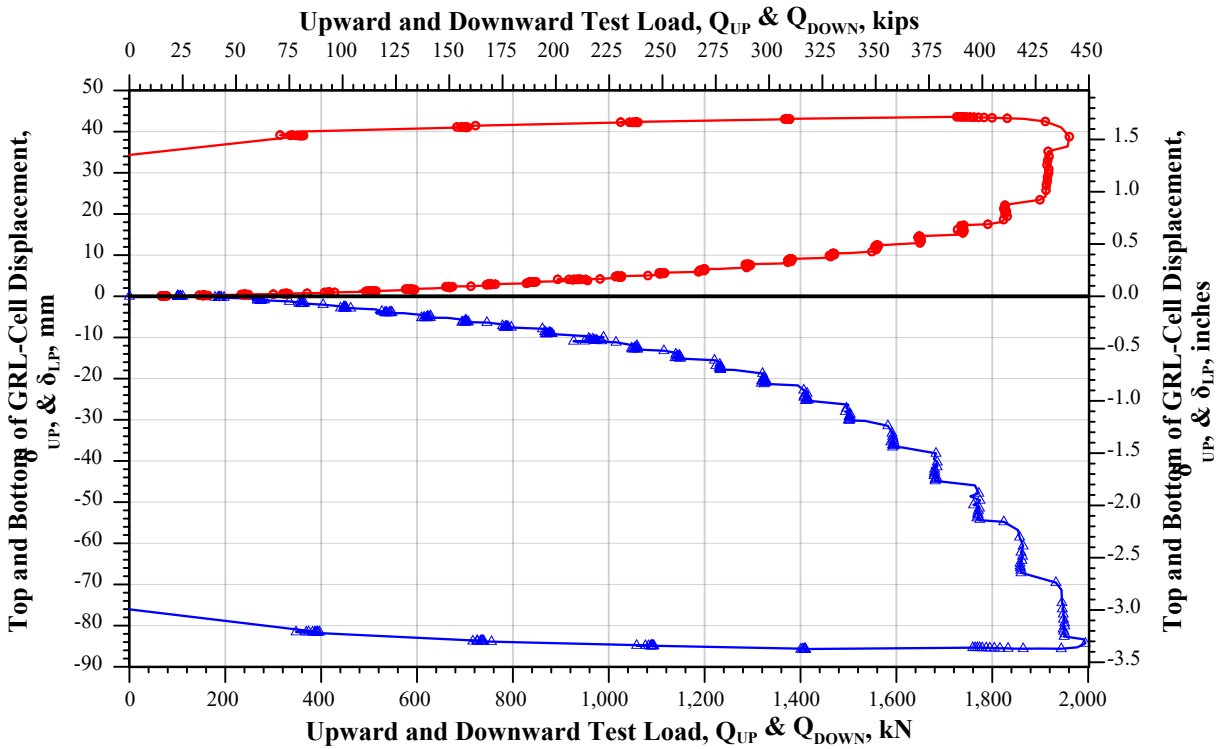


Figure 5. TACIP-1 jack assembly load-displacement plot.

As evidenced by significantly increasing displacement without corresponding increase in resistance, review of Figure 4 indicates full mobilization of side-shear resistance above the TDDP-1 jack assembly after the 867-kN (195-kip) loading increment, at an upward displacement of approximately 5.1 cm (2 inches). Combined nominal side-shear and end-bearing resistance below the jack assembly was only partially mobilized, as evidenced by limited downward movement. The maximum bi-directional test load achieved for TDDP-1 was 1,939 kN (436 kips), corresponding to GRL-Cell top and bottom displacements of 8.38 and 0.97 cm (3.30 and 0.38 in), respectively.

Better definition of greater mobilized resistances was obtained for TACIP-1, primarily resulting from improved approximation of the resistance balance point (and therefore the GRL-Cell location), and from applying a greater number of loading increments. General interpretation of Figure 5 indicates nearly full nominal resistance mobilization above and below the jack assembly. However, the limited resistance was activated above the GRL-Cell, negating any additional mobilized end-bearing resistance. The maximum bi-directional test load achieved for TACIP-1 was 3,954 kN (889 kips), corresponding to GRL-Cell top and bottom displacements of 8.43 cm (3.32 inches), respectively.

It should be noted that an increased number of loading increments not only provide better definition of the load-displacement curves, subsequent data reduction (requiring assessment of changes in applied loads and strains) is significantly improved with a greater number of equal loading increments. It is therefore recommended to establish the test loading schedule with a minimum of 20 equal loading increments, if possible. Special consideration of the jack assembly

location, embedded SG levels' locations, and pile-end effects in response to applied test loads (i.e., pile head response to upward load application, and pile base response to downward load application) should be taken into account when planning the testing program (Komurka and Moghaddam, 2020; Komurka and Robertson, 2020).

Data Reduction Methodology for Converting Strain to Internal Force. The American Concrete Institute (“ACI”) relationship which estimates grout modulus based on unconfined compressive strength (ACI, 2014), and the Incremental Rigidity (“IR”) method (Komurka and Moghaddam, 2020) were each evaluated for use in converting measured strains to calculated internal forces. The internal force at each strain gage level is critical to computing unit side-shear resistance along a pile’s embedded length, which is equal to the difference in boundary forces (i.e., internal forces and boundary conditions) divided by the pile area in contact with geomaterial. Difficulty arises in accurately computing internal force due to uncertainty in determining grout elastic modulus (E_{GROUT}), as internal force is proportional to measured strain by the pile’s axial rigidity (EA).

Grout elastic modulus is generally recognized as a strain-dependent property; however, a commonly used approach employing an empirical formula assumes a constant, strain-independent correlation between E_{GROUT} and grout uniaxial compressive strength (f_c'). Practitioners often rely on a relationship outlined by ACI (2014) which is better-suited for concrete (i.e., $E_{\text{CONCRETE}} (\text{psi}) = 57,000\sqrt{f_c'}$). This correlation can be reduced up to 25% as stated in ACI (2014) for lightweight concrete, and it is generally understood that E_{GROUT} is less than that of concrete for an equivalent axial compressive strength (Brown et al., 2007; Hassan et al., 1998). However, there are limited studies available for providing reliable correlation between f_c' to E_{GROUT} , nor are alternative methods for determining strain-dependent moduli of grout and concrete routinely implemented.

The Incremental Rigidity method utilizes changes in embedded strain gage measurements and applied loads to independently compute the strain-dependent pile rigidity at each interpretable strain gage level, permitting a more-direct method of converting strain to internal force. The underlying theory is summarized by Komurka and Moghaddam (2020), and several case studies are discussed for practical application to static load tests on drilled and driven deep foundations by Komurka and Robertson (2020). Limitations to applying this method exist; for example, for some soil conditions and associated geo-structural failure mechanisms, and inadequately applied static loading increments (Komurka and Robertson, 2020).

Initial review of the BDSLT measurements for TDDP-1 yielded uninterpretable data for direct application of the IR method. Therefore, without any laboratory tests to determine E_{GROUT} directly, strain-to-force conversion utilized the ACI formula. Improved loading schedule incorporating more load increments prior to failure, and better positioning of each strain gage level relative to the applied load contributed to the appropriateness of applying the IR method to TACIP-1 strain data. For the purposes of this study, and for consistency in results' comparison between the two test piles (given their similarities in cross-sectional area, grout mix design, and reinforcing cage design), back-calculated strain-dependent rigidity response from TACIP-1 at combined SG Levels B1 and B2 using the IR method were applied to both test piles. Figure 6 displays the strain-

dependent IR relationship, and also displays the strain-independent rigidity determined using the ACI formula for comparison. Based on these results, strain-dependent grout moduli were deduced for computing internal forces at each strain gage level for both test piles. The computed internal forces versus elevation at the maximum achieved test load for each test pile are displayed in Figure 7.

Load Transfer Results. Given each pile was installed to a different pile base elevation, direct comparison of end-bearing resistance is not necessarily meaningful. Accordingly, TDDP-1 and TACIP-1 responses are examined from the load transfer mechanisms in side-shear resistance. Load transfer refers to the manner in which loads applied to the foundation are resisted by the surrounding geomaterial, and is determined from the difference in boundary forces divided by the respective shaft area between those boundaries. Boundary forces are determined from the aforementioned calculated internal forces at each strain gage level, the pile head (i.e., internal force is zero), and the applied GRL-Cell test loads. The pile side area in contact with soil was determined from the TIP-generated pile profiles.

The unit side-shear resistances (t) are conventionally plotted as a function of relative pile-soil displacement (z), oftentimes referred to as t - z curves. Similarly, end-bearing resistances are conventionally plotted as a function of base movement (z_{BASE}), and are oftentimes referred to as $Q_{BASE-z_{BASE}}$ (total resistance, force units) or $q_{BASE-z_{BASE}}$ (unit resistance, force per unit area units) curves. Herein, residual side-shear/end-bearing resistance is referred to as no additional increase in soil resistance with increasing pile/soil relative displacement. The t - z and $q_{BASE-z_{BASE}}$ curves for each test pile are displayed in Figures 8 and 9, respectively.

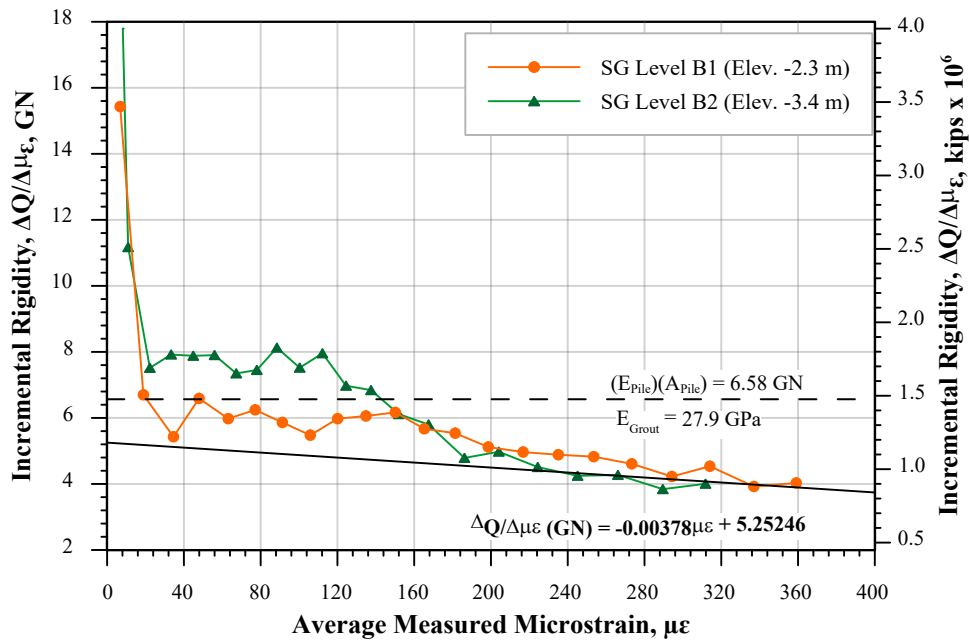


Figure 6. Incremental Rigidity versus Strain for interpretable SG Levels in TACIP-1.

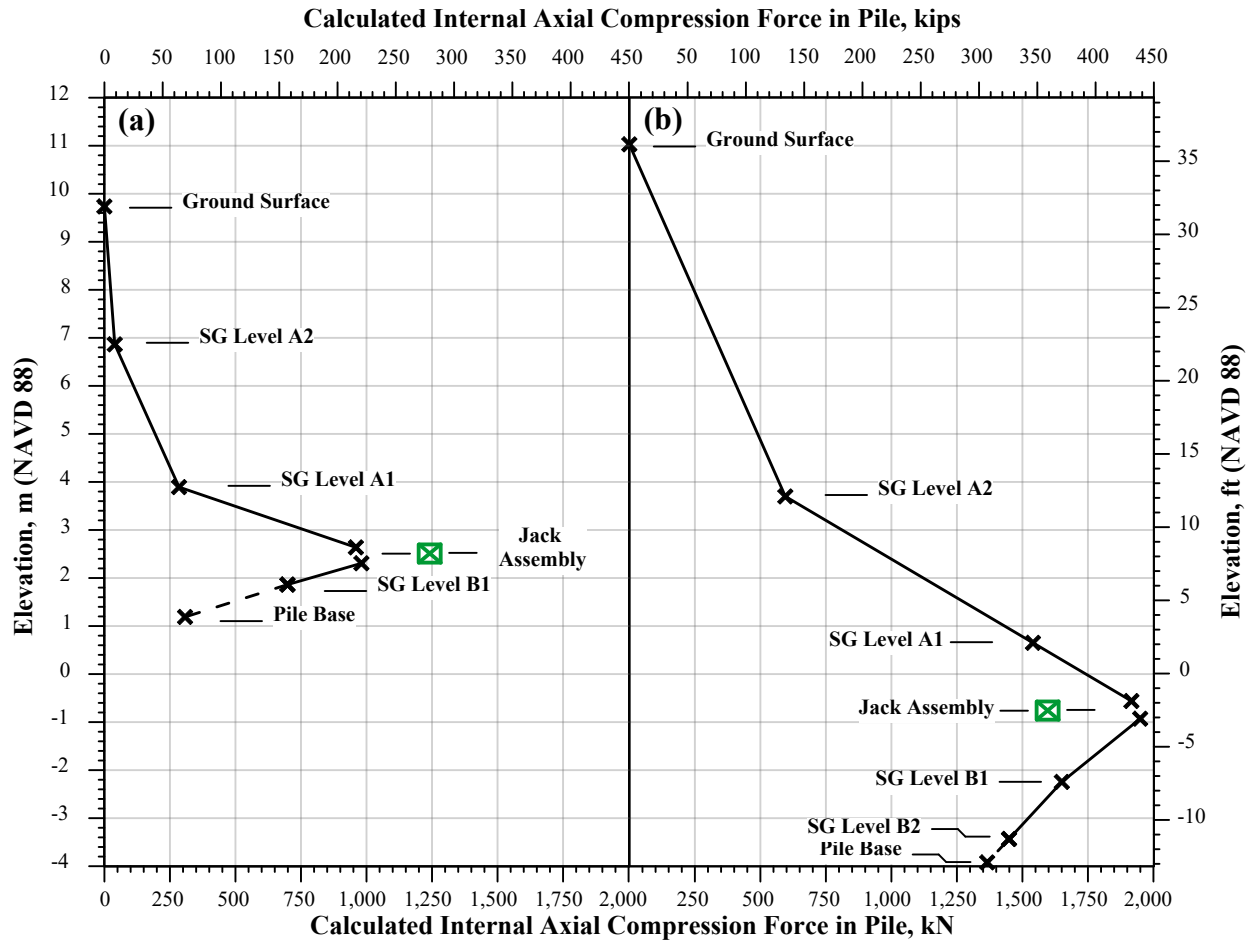


Figure 7. Internal force profiles at the maximum achieved bi-directional test load for (a) TDDP-1, and (b) TACIP-1 using the IR method.

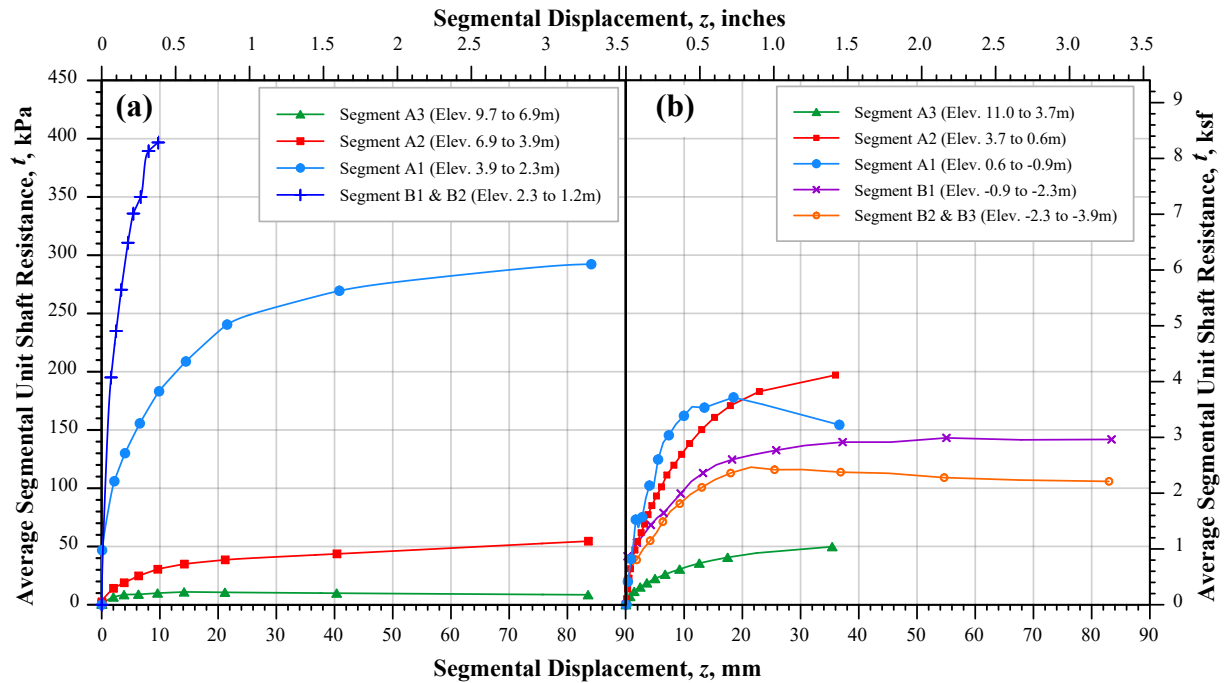


Figure 8. Load transfer results, displaying t - z curves for (a) TDDP-1, and (b) TACIP-1.

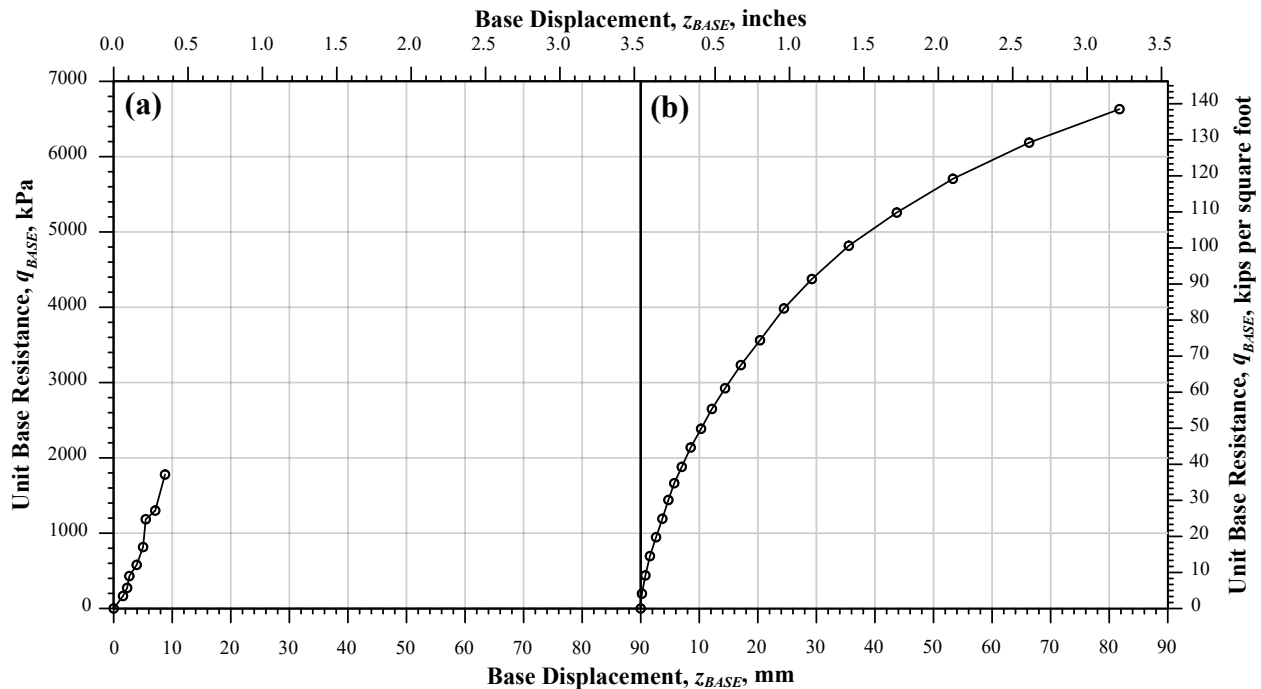


Figure 9. Load transfer results displaying q_{BASE} - z_{BASE} curves for (a) TDDP-1, and (b) TACIP-1.

COMPARISON OF LOAD TEST RESULTS ON TDDP-1 AND TACIP-1

A review of Figure 8 indicates that based on the load transfer results, full mobilization of nominal side-shear resistance was exhibited for most pile segments along each test pile. The exceptions were for the side-shear and end-bearing resistances below the jack assembly for TDDP-1, and the TACIP-1 end-bearing resistance (albeit more than 7.6 cm (3 in) of base displacement indicates that the nominal end-bearing resistance was likely nearly mobilized). Table 1 presents a comparison of the peak and residual (if achieved) side-shear resistance calculated for each pile segment.

Load transfer results for both test piles can be isolated for 1) the fill material, organic soil, and upper silty sand (extending from ground surface to Elevation 3.7 m (12.1 ft), and 2) the poorly graded sand with gravel (glacial deposits extending to Elevation 0.6 m (2.1 ft). The unit side-shear resistances in the upper soils were similar for each test pile, where the maximum mobilized resistance was approximately 47.9 kPa (1.0 ksf). Higher unit side-shear resistances were evidenced along TDDP-1 in the glacial deposits, ranging from 292.1 to 397.4 kPa (6.1 to 8.3 ksf) compared to 196.3 kPa (4.1 ksf) in the same material along TACIP-1. Side-shear resistances at greater depths along TACIP-1 ranged from 105.3 to 177.2 kPa (2.2 to 3.7 ksf), less than the resistances observed at higher elevations along TDDP-1. It should be noted that the calculated side-shear resistances for the TDDP-1's Segments B1 and B2 are uncertain due to the close proximity of the strain gages to the applied load location.

Table 1. Comparison of Unit Side-Shear and End-Bearing Resistances

Test Pile	Segment	Segment Elevation, m (ft)		Soil Description	Peak / Residual Mobilized Unit Resistance, kPa (ksf)
		Top	Bottom		
TDDP-1	A3	9.7 (31.9)	6.9 (22.5)	Fill material over organic soil	9.6 (0.2) / 9.6 (0.2)
	A2	6.9 (22.5)	3.9 (12.8)	Organic soil over silty sand	52.7 (1.1) / 52.7 (1.1)
	A1	3.9 (12.8)	2.3 (7.7)	Silty sand over poorly graded sand with gravel	292.1 (6.1) / 292.1 (6.1)
	B1 & B2	2.3 (7.7)	1.2 (3.9)	Poorly graded sand with gravel	397.4 (8.3) ^{1,2}
	Shaft Base	-----	1.2 (3.9)	Poorly graded sand with gravel	1,776.4 (37.1) ^{1,2}
TACIP-1	A3	11.0 (36.2)	3.7 (12.1)	Fill material, organic soil, over silty sand	47.9 (1.0) / 47.9 (1.0)
	A2	3.7 (12.1)	0.6 (2.1)	Silty sand over poorly graded sand with gravel	196.3 (4.1) / 196.3 (4.1)
	A1	0.6 (2.1)	-0.9 (-3.0)	Poorly graded sand	177.2 (3.7) / 153.2 (3.2)
	B1	-0.9 (-3.0)	-2.3 (-7.4)	Poorly graded sand	143.6 (3.0) / 143.6 (3.0)
	B2 & B3	-2.3 (-7.4)	-3.9 (-12.9)	Poorly graded sand with silt	119.7 (2.5) / 105.3 (2.2)
	Shaft Base	-----	-3.9 (-12.9)	Poorly graded sand with silt	6,631.4 (138.5) ¹

Notes:

1. Nominal resistance was not fully mobilized.
2. Unit resistances are uncertain due to the close proximity of the strain gages to the applied load location.

Nevertheless, it can be concluded that the DDP achieved a limited increase in unit shaft resistance compared to the ACIP pile in both the loose granular and organic soil deposits. The DDP achieved a 50 to 100% increase in unit side-shear resistance compared to the ACIP pile in the dense mixed granular deposit. Due to differences in the piles’ base elevations and lack of full end-bearing resistance mobilization, no direct indication of potential soil improvement effects on end-bearing resistance for the DDP compared to the ACIP pile can be inferred.

Despite the difference in each piles’ embedded length, another means of response comparison is accomplished by estimating the piles’ top-displacement curves. An Equivalent Top-Loading (“ETL”) curve was generated for each test pile using the load-transfer method, which incorporates the computed $t-z$ and $Q_{BASE}-z_{BASE}$ curves assuming the pile response is independent of the direction of applied load. The ETL curves were computed using TZPILE software from Ensoft, Inc.. Foundation base displacements under top-loading conditions were prescribed, and the load at the pile head was determined using an iterative process. The ETL analysis was carried out to a prescribed base movement corresponding to the maximum measured base displacement, and therefore the maximum modelled pile head load does not necessarily reflect the maximum achieved bi-directional test load. The ETL curves are displayed in Figure 10. The primary conclusion from this comparison is that relatively similar estimated pile-top load-displacement response was modelled up to a 1,670-kN (375-kip) top load, with a slightly stiffer response from the longer ACIP pile. However, significant limitation in the achievable DDP capacity was evident due to the restricted maximum embedment depth in dense glacial deposits.

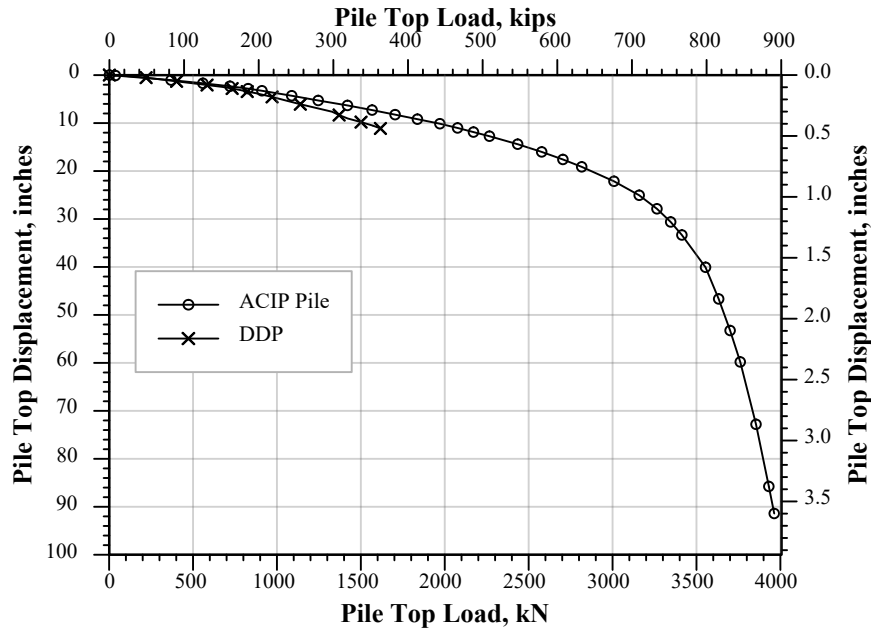


Figure 10. ETL Curves Comparison.

SUMMARY AND CONCLUSIONS

This construction project in the Pacific Northwest incorporated bi-directional static load testing on two sacrificial test piles: an 8.5-m (28-ft) long DDP embedded 2.0 m (6.5 ft) into dense glacial deposits, and a 14.9 m (49-ft) long ACIP pile embedded 7.1 m (23.4 ft) in dense glacial deposits. The shorter DDP embedment reflected the limitation of the installation method in dense granular materials, as the pile was drilled to auger refusal. A close examination of load test data reduction methods, specifically converting measured strain to calculated internal forces, was discussed for consistency between each test pile’s results. Based on load test results and comparison of the two pile installation methods, several conclusions can be made:

1. For this case study, the maximum achievable embedment from the DDP was limited to approximately 2 m (6.5 ft) into dense granular glacial till strata (roughly 4 to 5 pile diameters). No limitation in drilling penetration into this stratum was realized with the ACIP pile.
2. Pre-planning of SG levels and proper loading schedule helps improve data reduction for more-direct conversion of strain to internal force utilizing the Incremental Rigidity method. Commonly, industry practice relies on semi-empirical relationships (i.e., the ACI formula) for establishing critical pile properties required for interpreting strain measurements, which may result in a significant misrepresentation of grouted-pile internal forces. Owing to the strain-dependent modulus response of grout, use of the Incremental Rigidity method provided more-accurate internal force profiles and unit side-shear resistances for both test piles.
3. An approximate 50 to 100% increase in nominal unit side-shear resistance was observed in a dense granular deposit with DDP verses ACIP pile installation methods. The side-

shear resistance calculated in the dense glacial deposits ranged from 292.1 to 397.4 kPa (6.1 to 8.3 ksf) for TDDP-1, and was 196.3 kPa (4.1 ksf) for TACIP-1. No significant difference in nominal side-shear resistance between the test piles was computed in the upper deposits, which consisted of fill materials, organic soils, and loose silty sand.

4. While higher unit soil resistances can be achieved with DDPs due to soil improvement effects surrounding the pile, limitations in the construction method may manifest as relatively shallow drilling-tool refusal, limiting the maximum achievable total pile capacity.

ACKNOWLEDGEMENTS

The authors would like to extend their appreciation to Malcolm Drilling Company, Inc., the drilling contractor on the case study examined herein, for allowing us to present the information and results obtained on this test program.

REFERENCES

- ACI Committee, American Concrete Institute, & International Organization for Standardization (2014). Building Code Requirements for Structural Concrete (ACI 318-14) and Commentary. American Concrete Institute.
- Basu, P., Prezzi, M., and Basu, D. (2010). “Drilled Displacement Piles – Current Practice and Design.” *DFI Journal*, Vol. 4, No. 1, August 2010.
- Bixler, M., Belardo, D., Piscalko, G. (2016). “Case Histories Utilizing Thermal Integrity Profiling for Foundation Quality Assurance.” *GeoVancouver 2016*, Vancouver, BC, Canada.
- Brown, D. (2012). “Recent Advances in the Selection and Use of Drilled Foundations.” *ASCE GeoCongress 2012*, Oakland, California.
- Brown, D., Dapp, S., Thompson, R., and Lazarte, C. (2007). “Design and Construction of Continuous Flight Auger Piles.” Geotechnical Engineering Circular No. 8, Federal Highway Administration.
- Hassan, K.M., O’Neill, M. W., and Vipulanandan, C. (1998). Specification and Design Criteria for the Construction of Continuous Flight Auger Piles in the Houston Area.” Report No. UH 3921-1, Texas Department of Transportation, pp 85.
- Komurka, V.E., and Moghaddam, R.B. (2020). “The Incremental Rigidity Method – More-Direct Conversion of Strain to Internal Force in an Instrumented Static Loading Test.” *ASCE GeoCongress 2020*, Minneapolis, MN.
- Komurka, V.E., and Robertson, S. (2020). “Results and Lessons Learned from Converting Strain to Internal Force in Instrumented Static Loading Tests Using the Incremental Rigidity Method.” *ASCE GeoCongress 2020*, Minneapolis, MN.

Park, S., Roberts, L.A., and Misra, A. (2011). “Static load test interpretation using the t - z model and LRFD resistance factors for auger cast-in-place (ACIP) and drilled displacement (DD) piles.” *Int. Journal of Geotechnical Engineering*, Vol. 5, pp 283-295. DOI 10.3328/IJGE.2011.05.03.283-295.

Piscsalko, G. (2014). “Non-Destructive Testing of Drilled Shafts and CFA Piles – Current Practice and New Method.” *Proceedings of the DFI/EFEC Int. Conf. on Piling and Deep Foundations*, Stockholm, Sweden.